2022 44th Annual International Conference of
the IEEE Engineering in Medicine & Biology Society (EMBC)
Scottish Event Campus, Glasgow, UK, July 11-15, 2022

2022 44th Annual International Conference of the IEEE Engineering in Medicine & Biology Society (EMBC) | 978-1-7281-2782-8/22/$31.00 ©2022 IEEE | DOI: 10.1109/EMBC48229.2022.9871936

An Impedance Sensor for Pathologically Relevant Detection of In-Stent Restenosis *In Vitro*

Daniel Hoare, Simon Fisher, Finlay Nelson, Andreas Tsiamis, Jamie R. K. Marland, Srinjoy Mitra, Steve L. Neale, John R. Mercer

Abstract. **Cardiovascular disease (CVD) is the biggest cause of death globally. CVD is caused by atherosclerosis which is the accumulation of fatty deposits, often within the fine arteries of the heart or brain. These blockages reduce blood flow and lead to oxygen starvation (ischemia) which can lead to heart attacks and strokes. To treat blocked arteries an implantable device called a stent re-opens the artery to reinstate blood flow to the organ. The stent itself can become blocked over time by cell growth (intimal hyperplasia) which is characterised by excessive smooth muscle cell proliferation. Sensors based on electrical impedance spectroscopy (EIS) embedded in a stent could detect this re-blocking to allow for early intervention. Using platinum interdigitated electrodes on silicon sensor wafers we were able to co-culture different ratios of mouse smooth muscle cells and mouse endothelial cells on these sensors. This mimics the complex, multicellular environment which a stent is found in vivo when undergoing neo-intimal hyperplasia. Trends in the cell impedances were then characterised using the detection frequency and the gradient of change between populations over time which we termed 'Peak Cumulative Gradients (PCG). PCGs were calculated to successfully discriminate each cell type. This work moves towards a sensor that may help guide clinician's decision-making in a disease that is historically silent and difficult to detect. *Clinical Relevance*— This moves towards an early warning system for the detection of neo intimal hyperplasia ultimately leading to a reduction in stent complications.**

I. Introduction

The largest cause of death in the world is cardiovascular disease (CVD), resulting in 1 in 3 deaths globally.[1] The disease is underpinned by atherosclerosis which is the progressive accumulation of fibrofatty and vascular smooth muscle cell (VSMC) deposits within an artery [2]. Common risk factors such as smoking, a lipid rich diet coupled with hypertension are major risk factors that promote inflammation that drive loss of the fine endothelial intimal layer that separates the vessel wall from the blood stream.[3] Overtime atherosclerotic plaque will restrict blood flow and, in some cases, completely block the artery. Within the fine coronary arteries of heart this will lead to a myocardial infarction (MI) or stroke within the cerebral circulation of the brain.

To treat this an implantable medical device (IMD) called a stent is used in conjunction with a procedure called percutaneous coronary intervention (PCI). A PCI aims to restore patency and blood flow back to the blood vessel.[4] In order to achieve this catheters are inserted into and through the peripheral vasculature, usually the radial or femoral artery, to the site of disease. A balloon is passed across the blockage and expanded which in turn pushes back the fatty deposit into the wall of the vessel. In order to maintain vessel patency a stent is expanded which locks in place to stops the fatty blockage recoiling back into the blood. Stents have been a major success in the treatment of atherosclerosis with over 3 million placed in the USA, Europe and China every year but come with limitations. A particularly vindictive complication is a wound response that induces vascular smooth muscle cell (VSMC) hyperplasia termed in-stent restenosis (ISR).

In-stent restenosis is the reblocking of a stent, and vessel by the excessive proliferation of VSMCs. It is caused when the stent damages the fine endothelial lining of the artery causing endothelial dysfunction and exposing the medial layer of the artery to the bloodstream. In response VSMCs are able to proliferate across the stent and into the lumen of the artery.[5] This hyperplasia is accelerated by an inflammatory cascade that drives recruitment of monocyte/macrophages.[6,7]

One type of sensor to achieve this is electrical impedance sensing (EIS) which comprises of an alternating current being passed across electrodes. As cells settle, adhere and proliferate across the electrodes the current is resisted which leads to an increase in the electrical impedance (Z-Ohms).[8,9] To date alternative "Smart Stents" have been designed with the focus on pressure measurements with novel sensors and their own integration method to a stent. [10,11] These implantable medical devices (IMDs) have the ability to show long term pressure changes however the minute change early on in ISR cannot be addressed as flow and pressure interactions develop late. Intervention usually involves a second invasive procedure. Previously, our group developed a therapeutic interdigitated electrode capable of detecting cell growth while also inducing cell death in a controlled manner called apoptosis. However, we had yet to developed a senor

*Research supported by Supported by the Engineering and Physical Sciences Research Council and by the doctoral training program from the University of Glasgow, EP/S515401/1.

D. Hoare, S. Fisher and J. R. Mercer are with the Institute of Cardiovascular & Medical Sciences, University of Glasgow, Glasgow, UK (corresponding author J. R. Mercer ; e-mail: john.mercer@glasgow.ac.uk.

A. Tsiamis, J R. K. Marland and S. Mitra is with the Institute for Intergrated Micro and Nano Systems, University of Edinburgh, Edinburgh, UK.

S. L. Neale and F. Nelson is with the School of Engineering, University of Glasgow, Glasgow, UK.

to a physiologically relevant size, previously 200,000 μm^2 area. nor had we assessed the sensor in tissues similar to that of an artery.

In this paper we address these limitations by investigating the sensors response to cellular components closely related to the constituents of a vessel wall under. We do this through the use of co-culturing primary mouse endothelial cells (MECs) and mouse aortic smooth muscles cells (MASMCs) in differing ratios. Unlike isolated cell populations which are not found in physiological conditions these cocultures better simulate the sensors detection of ISR as an *in vitro* representation of the short term consequences of endothelial disruption and VSMC hyperplasia found *in vivo*.

II. Methods

A. Sensor and Chamber Fabrication

Silicon sensors with platinum IDEs were fabricated as previously described.[12] This created platinum interdigitated electrodes on a silicon substrate covering a 2,500 μm^2 area. A Perspex chamber was attached over each sensor, sterilised with 70% ethanol and rinsed thrice with de-ionised water before cell seeding and impedance measurements made.

B. Culturing of Cells

Pure MASMCs and MECs were cultured as previously described.[13,14] Co-cultured cells were initially incubated and grown to these same conditions separately before being combined. Each cell type was counted using a haemocytometer and the total number of cells calculated. From this a percentage share of each cell was calculated with a maximum number of cells per a device being 50,000. For example, to seed a chamber containing 70% MEC and 30% MASMC a density of 35,000 MEC and 15,000 MASMC were seeded in a total volume of 800µL of culture media. Measurements were taken at 1 hour intervals for 24 hours.

C. Fluorescent Cell Staining

Cells were stained using Calcein AM (green) and Calcein red orange (red) (Invitrogen, Thermo Fisher Scientific, USA, C34851 and C3100MP). Trypsinised cells were neutralised with media (Dulbecco′s Modified Eagle′s Medium, DMEM, HEPES Gibco, Thermo Fisher Scientific, USA) and pelleted at 1000 rpm for 5 minutes. The media was removed and the pellet was washed and resuspended with 200 µL phosphate-buffered saline (PBS) (Gibco, Thermo Fisher Scientific, USA, 14190144) before being pelleted a second time to remove all traces of serum, the PBS was then removed. 2 µL of dye was dispersed with 198 µL of culture to a final concentration of 10 µM. MECs were stained green and MASMC stained red. Cells were incubated for 30 minutes before a third pellet was formed and dyes were removed. Cells were resuspended in culture media and the cells were counted and seeded.

D. Impedance Measurements

Impedance measurements were made at 30 minutes intervals using a Hioki IM3536 LCR meter, accuracy ±0.05% with a resolution between 4 Hz to 8 MHz of 5 digits and a minimum resolution of 10 mHz. A frequency range of 1kHz to 1MHz was used to interrogate the device. A constant current setting of 10 µA was used. Impedance, phase angle and reactance were recorded from the instruments to a laptop where files were formatted allowing for statistical analysis.

E. Imaging

Olympus BX51 with CoolLED fluorescent light source was used to image the device a QImage camera. Digital images were acquired using the QImage Pro software suite. Overlays were created using ImageJ open-source software with no additional plugins.

F. Data Organisation and Statistical Analyses

Normalisation of the data was performed by ratioing of the change from 0 hours per a repeat at each time point across the frequency spectrum. Normalised data was then parsed into Python (3.8) using Pandas (1.0.3). These data were then sub-set to sweeps between 10 and 12 hours. Numpy (1.19.5) was used to calculate the gradient of the sweep and these gradients were then filtered to measurements where the impedance gradient was >0.02 Ω/Hz creating a new array of positive gradients. All values within the new array were summed, returning a single value referred to as 'Peak Cumulative Gradient' (PCG), where this value represented the magnitude of the upstroke of the sweep. Data was visualised using Matplotlib via Seaborn (0.11.1).

Within group normality was verified using the Shapiro-Wilk test using Pingouin (0.3.12). A total of 4 from 70 (5.7%) measurements were derived from erroneous technical measurements and thus were labelled as NaNs within the data. These NaN measurements were then imputed using Sklearn_Iterativeimputer (0.24.2), a median based multivariate imputation algorithm which derives imputation from both within and between group methods. As sensors were paired, Pingouin (0.3.12) was used to perform pairwise t-tests. Returned p-values were corrected for multiple testing using the Benjamini-Hochberg false-discovery-rate (FDR) correction. Additional, graphing, area under the curve analysis and unpaired t-tests for blood versus clot and stent-sensor control versus stent-sensor cells were performed with GraphPad Prism 9.

III. Results

A. Seeding Density Control and Monolayer Formation

In seeding a co-cultured mixed population, the initial seeding uniformity was calculated to observe if the prescribed ratio of cells equated to that required, figure 1. Fluorescent images analysed from representative fields shown in figure 1B-D allowed the number of MASMC (red) and MEC (green) to be calculated. This was expressed as a ratio of MASMC to MEC with the ratio of MASMC reported in figure 1A. Between the groups a significant difference can be observed at the different ratios. After 24 hours of incubation each repeat was checked for monolayer formation.

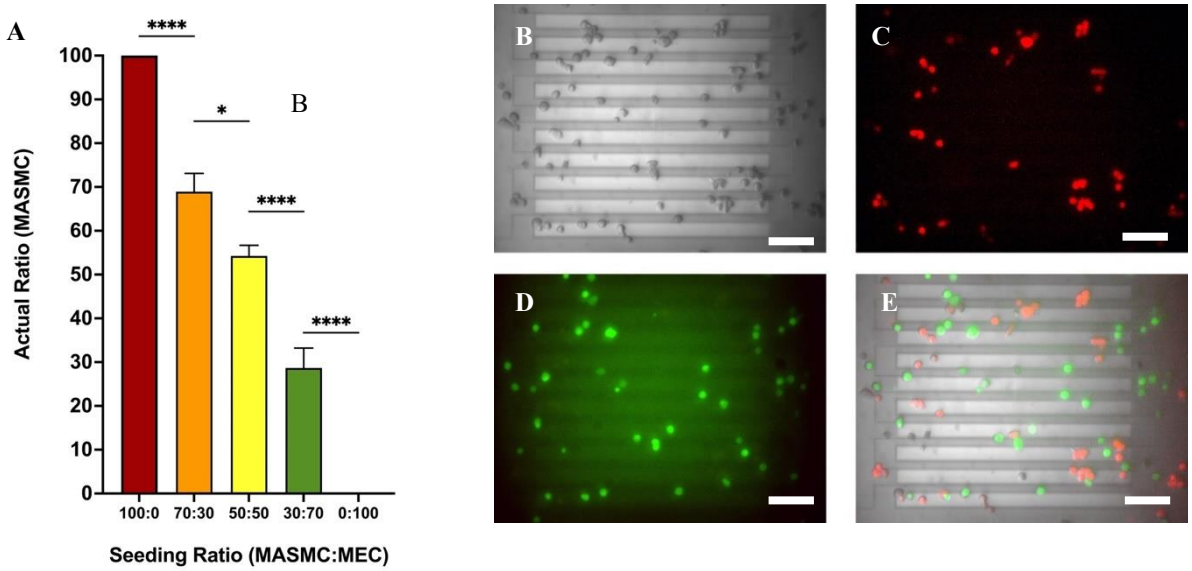

Figure 1 *– Seeding density control of each cell type. Panel A shows the mean ratios of cells for each density. The right-side images show example of seeding count for a 50:50 MASMC red and MEC green. Panel B shows the bright field, Panel C shows the MASMC dyed with C34851, Panel D shows the MEC dyed with C3100MP and Panel E shows the merge of B,C and D. Scale bar is 100µm. N=7, mean with SEM, * = <0.05, ****=<0.0001*

B. Impedance Analysis

Using the LCR meter we measured both the impedance of the cell populations at 1 hours intervals for 24 hours using a 1kHz to 1MHz frequency sweeps. The change from each repeat's 0 hours baseline was used to normalise the data before the PCG of the impedance was calculated, see methods. A control of media only was used to assess that all cell populations were in fact causing impedance changes, versus control all cell populations were significantly different at the time points investigated. Analysis of the PCG for the growth of isolated MECs and MASMCs and co-cultured populations across the sensor returned a non-linear, 'J-shaped' relationship, for impedance, respectively figure 2. Importantly, the MASMC 100% culture has generally higher impedance than the 100% MEC, with the former having significantly greater PCG, indicating a higher and more sustained upstroke of the sweep. Interestingly, co cultured 50:50 MASMC:MEC seeded across the sensor returned significantly lower PCG versus either of the pure populations. In summary, by using measurements of PCG, we are able to observe trends in the presence of different ratios of cells on sensor, however, this relationship is multivariate and non-linear.

IV. Discussion

Integrating bioelectronic sensors into existing implantable medical devices will fundamentally change the way patients and clinicians obtain clinical data. The complex characteristics of the *in vivo* environment has led us to model these cell sensor interactions through the use of *in vitro* techniques. In this work we have shown the sensors ability to gather data that could be predictive of the cell types present on the sensor allowing for an early warning prediction and a long-term assessment tool. We believe this to have significant clinical advantage over current stents used to treat atherosclerosis as well as meeting limitations of other Smart Stents currently being researched. Using the stent as an integrated antenna with a pressure sensor attached researchers were able to wirelessly detect pressure changes.[15] This was progressed to have *in vitro* and *in vivo* experiments including a therapeutic addition via resonant heating of the stent. [11,16] Similarly, a wireless pressure sensor integrated into a 3D printed stent was able to detect pressure changes from within a stent under bench testing.[17,18] A detection of 60% percent occlusion on bench was also shown through a fully integrated pressure stent system.[19] As discussed recently the choice between a re-stenting or a coronary artery bypass graft is confirmed by the percentage occlusion, with 50-70% depending on the vessel.[20] Indeed these devices are capable

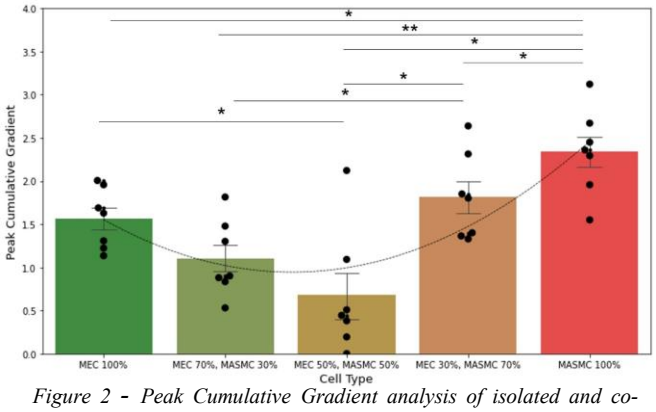

*Figure 2 - Peak Cumulative Gradient analysis of isolated and co-cultures MASMC:MEC populations seeded onto silicon sensors. Cells were maintained over 24 hour period. Peak Cumulative Gradient is measured in arbitrary units of gradient change. Dotted line shows the 2nd order polynomial fit over a linspace of 400 within the dimensions of the data. Error bars indicate the standard error of the mean (SEM), dots show individual data-points, bar height indicates group mean. Sensors were paired between seeding densities, * = p< 0.05 (FDR adjusted), ** = p < 0.01 (FDR adjusted), pairwise t-test. N=7*

of detecting this however at this point an intervention is needed. Our device is capable of detecting ISR in its earliest form when a monolayer of a few cells thick is growing. The main advantage of our device is this early detection that can then inform the physician to use our therapeutic intervention to induce apoptosis therefore negating the need for a secondary intervention. It must be noted that following PCI secondary lesions outside of the stents sphere of influence can occur and would not be detectable by this system. Therefore, further sensors or calibration/redesign of the sensors to detect flow and biomarkers within the device could help detect lesions outside of the area of the stent.

The use of an impedance sensor for this detection has previously been shown however not integrated into to a stent. Holland *et al* grew monolayers for varied time lengths from porcine endothelial and smooth muscle cells measuring the impedance over time. Similarly to our work they showed distinct changes in the impedance of the cell types across a frequency range of 1kHz to 100 kHz.[21] Unlike our work the SMCs was lower than that of the ECs however these were different animals which will ultimately have an effect on the impedance. Here we are able to build on this work by using mixed populations to show that the presence of both cell types causes a marked change in impedance. PCG seemed to be particularly well suited to the cell detection process because of the analysis of changes across a spectrum of data in relation to time.

We hypothesised a linear relation between the ratio of MASMC and the magnitude of impedance. By normalising the frequency spectrum, we were able to observe the frequencies where the most deviation form 0 hours in each sample was apparent and the analyse this for all samples. By using the PCG, we do not limit samples to a single frequency and can more easily track change over time as a change in spectral frequency as a cell signature, even for mixed cell populations. In doing this the trend in the data is in actuality a J shape curve was noticed between the MEC and MASMC as the ratios differed. In growing a monolayer across the sensor, a barrier forms that impedes the flow of current. Previously the compactness, health and adherence of the monolayer was shown to affect the impedance by adding drugs to the monolayer.[9,22–24] In our experiment we observe a similar effect however this is through the addition of different ratios of cells. Proliferative SMCs, such as those used in this experiment, have an inhibitory effect on endothelial cells, reducing proliferation of the cells.[25,26] As such by introducing them to a co-culture of MECs the monolayer formed will not be that as strong as MECs alone while the MECs will have a similar effect on the MASMCs in these experiments. When the MASMCs and MECs are in equal proportions formation of a confluent monolayer that is compact and strongly adhered to the surface is hard to form and as such the impedance gradient drops, see figure 2. By performing this study, we believe that moving into an *in vivo* model will result in more comparable results than single cell monolayer alone. However, the changes when moving from *in vitro* to *in vivo* are still expected.

V. Conclusion

In achieving a monolayer formation with co-cultured cells and detecting impedance changes we come closer to an early warning system for in stent restenosis. The use of co-cultured populations presents are more physiological condition for the sensor. The trends produced by PCG are promising that even within an *in vivo* the transition from healthy endothelial monolayer coverage of a stent could be distinguished from proliferative VSMCs allowing intervention form the earliest stage.

References

[1] WHO, *WHO* **2017**.
[2] P. Libby, *Nature* **2021**, *592*, 524.
[3] P. Libby, *Clin. Chem.* **2021**, *67*, 131.
[4] P. F. Ludman, *Medicine (Baltimore)*. **2018**, *46*, 547.
[5] N. Pal, J. Din, P. O'Kane, *Interv. Cardiol. (London, England)* **2019**, *14*, 10.
[6] S. O. Marx, H. Totary-Jain, A. R. Marks, *Circ. Cardiovasc. Interv.* **2011**, *4*, 104.
[7] C. Chaabane, F. Otsuka, R. Virmani, M.-L. Bochaton-Piallat, *Cardiovasc. Res.* **2013**, *99*, 353.
[8] P. Mitra, C. R. Keese, I. Giaever, *Biotechniques* **1991**, *11*, 504.
[9] I. Giaever, C. R. Keese, *IEEE Trans. Biomed. Eng.* **1986**, *BME-33*, 242.
[10] S. R. Green, R. S. Kwon, G. H. Elta, Y. B. Gianchandani, *Biomed. Microdevices* **2013**, *15*, 509.
[11] J. Chen, Y. Yi, M. Selvaraj, K. Takahata, *Sensors Actuators A Phys.* **2019**, *297*, 111527.
[12] J. Marland, M. E. Gray, C. Dunare, E. O. Blair, A. Tsiamis, P. Sullivan, E. González-Fernández, S. N. Greenhalgh, R. Gregson, R. E. Clutton, M. M. Parys, A. Dyson, M. Singer, I. H. Kunkler, M. A. Potter, S. Mitra, J. G. Terry, S. Smith, A. R. Mount, I. Underwood, A. J. Walton, D. J. Argyle, A. F. Murray, **2020**, DOI 10.31224/osf.io/fhqd7.
[13] J. Mercer, N. Figg, V. Stoneman, D. Braganza, M. R. Bennett, *Circ. Res.* **2005**, *96*, 667.
[14] J. Leiper, J. Murray-Rust, N. McDonald, P. Vallance, *Proc. Natl. Acad. Sci. U. S. A.* **2002**, *99*, 13527.
[15] K. Takahata, A. DeHennis, K. D. Wise, Y. B. Gianchandani, in *17th IEEE Int. Conf. Micro Electro Mech. Syst. Maastricht MEMS 2004 Tech. Dig.*, IEEE, **2004**, pp. 216–219.
[16] X. Chen, D. Brox, B. Assadsangabi, Y. Hsiang, K. Takahata, *Biomed. Microdevices* **2014**, *16*, 745.
[17] J. Park, J.-K. Kim, S. A. Park, D.-W. Lee, *Microelectron. Eng.* **2019**, *206*, 1.
[18] J. Park, J.-K. Kim, D.-S. Kim, A. Shanmugasundaram, S. A. Park, S. Kang, S.-H. Kim, M. H. Jeong, D.-W. Lee, *Sensors Actuators B Chem.* **2019**, *280*, 201.
[19] A. D. DeHennis, K. D. Wise, *J. Microelectromechanical Syst.* **2006**, *15*, 678.
[20] E. Z. Levy, in *2020 IEEE-EMBS Conf. Biomed. Eng. Sci.*, **2021**, pp. 230–235.
[21] I. Holland, C. McCormick, P. Connolly, *PLoS One* **2018**, *13*, e0206758.
[22] C. R. Keese, N. Karra, B. Dillon, A. M. Goldberg, I. Giaever, *Vitr. Mol. Toxicol. J. Basic Appl. Res.* **1998**, *11*, 183.
[23] J. A. Stolwijk, K. Matrougui, C. W. Renken, M. Trebak, *Pflugers Arch.* **2015**, *467*, 2193.
[24] I. Giaever, C. R. Keese, *Nature* **1993**, *366*, 591.
[25] C. S. Wallace, S. A. Strike, G. A. Truskey, *Am. J. Physiol. Circ. Physiol.* **2007**, *293*, H1978.
[26] B. Imberti, D. Seliktar, R. M. Nerem, A. Remuzzi, *Endothelium* **2002**, *9*, 11.